

# *In vivo* Estimation of Dispersion Anisotropy of Neurites Using Diffusion MRI

Maira Tariq<sup>1</sup>, Torben Schneider<sup>2</sup>, Daniel C. Alexander<sup>1</sup>,  
Claudia A.M. Wheeler-Kingshott<sup>2</sup>, and Hui Zhang<sup>1</sup>

<sup>1</sup> Centre for Medical Image Computing and Department of Computer Science,  
University College London, United Kingdom

<sup>2</sup> NMR Research Unit, Department of Neuroinflammation, Institute of Neurology,  
University College London, United Kingdom

**Abstract.** We present a technique for mapping dispersion anisotropy of neurites in the human brain *in vivo*. Neurites are the structural substrate of the brain that support its function. Measures of their morphology from histology provide the gold standard for diagnosing various brain disorders. Some of these measures, e.g. neurite density and orientation dispersion, can now be mapped *in vivo* using diffusion MRI, enabling their use in clinical applications. However, *in vivo* methods for estimating more sophisticated measures, such as dispersion anisotropy, have yet to be demonstrated. Dispersion anisotropy allows more refined characterisation of the complex neurite configurations such as fanning or bending axons; its quantification *in vivo* can offer new imaging markers. The aim of this work is to develop a method to estimate dispersion anisotropy *in vivo*. Our approach builds on the Neurite Orientation Dispersion and Density Imaging (NODDI), an existing clinically feasible diffusion MRI technique. The estimation of dispersion anisotropy is achieved by incorporating Bingham distribution as the neurite orientation distribution function, with no additional acquisition requirements. We show the first *in vivo* maps of dispersion anisotropy and demonstrate that it can be estimated accurately with a clinically feasible protocol. We additionally show that the original NODDI is robust to the effects of dispersion anisotropy, when the the new parameter is not of interest.

## 1 Introduction

Axons and dendrites, collectively known as neurites, are the projections from the cell body of a neuron; they are the structural underpinnings of brain functions. The morphology of neurites, quantified using histological analysis of postmortem tissue, provides the gold standard for understanding the development [1], function [2] and pathology [3] of the brain. Accessing such information non-invasively has been of great interest because this will enable a dynamic view of the brain in health and disease. Diffusion MRI (dMRI) is such a technique, which can probe the microstructure and is becoming an indispensable tool for assessing the structure of neurites, *in vivo*.

The standard dMRI technique, diffusion tensor imaging (DTI) [4], provides sensitivity to neurite morphology, but can not quantify specific measures such as neurite density and orientation dispersion. Jespersen et al. proposed the first dMRI technique to estimate these neurite measures directly [5] in *ex vivo* imaging; their technique was subsequently validated with detailed histological comparison [6]. Zhang et al enabled the *in vivo* mapping of these measures with the development of the neurite orientation dispersion and density imaging (NODDI) [7]. The clinical feasibility of NODDI has allowed the quantification of neurite morphology to gain adoption in neuroimaging research, e.g. to study epilepsy [8] and brain development [9].

However, one limitation of NODDI is that it can not characterise complex neurite configurations such as those arising from fanning and bending axons. NODDI models orientation distribution of neurites with the Watson distribution [10], which constrains the dispersion about the dominant orientation to be isotropic (see Fig.1). For fanning and bending axons, the dispersion about the dominant orientation is typically anisotropic: the dispersion is the highest along the plane of fanning and bending but the lowest perpendicular to the plane. *Ex vivo* imaging has shown such dispersion anisotropy is widespread in the brain [11] but can not be accessed with NODDI or other *in vivo* techniques. Quantifying this anisotropy *in vivo* will provide a more refined measure of neurite morphology that can serve as a potential imaging marker of neurite integrity [12] and be used to improve tractography [11,13].

The aim of this work is to develop a method that can estimate dispersion anisotropy of neurites *in vivo*. We take the approach of building on NODDI because it provides a dMRI acquisition protocol that has been demonstrated to be clinically feasible [8,9]. We propose a new NODDI model that incorporates the Bingham distribution [10] to enable the quantification of dispersion anisotropy of neurites. Bingham distribution has been used in various dMRI techniques [14,11], but the focus has been on mapping brain connectivity. Our aim is to map microstructure using biophysically meaningful parameters. The key advance in this work over these approaches is the use of multi-shell data, as in [7], which enables estimation of microstructure at the same time as the fibre dispersion parameters. Our proposed model enables estimation of dispersion anisotropy and the primary dispersion orientation, along with the estimates of

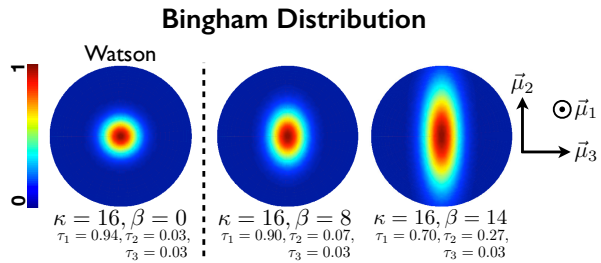


**Fig. 1.** Probability density plots for Bingham distribution. From left to right, increasing dispersion anisotropy about the dominant orientation  $\mu_1$ . The primary dispersion orientation,  $\mu_2$ , represents the orientation of dispersion anisotropy about  $\mu_1$ . Watson is a special case of Bingham distribution.

neurite density and their concentration along the dominant orientation, without imposing any additional acquisition requirements compared to the original model. We define a new measure of dispersion anisotropy based on the *Orientation Tensor* (OT), following the work by [12]. To assess the performance of the proposed NODDI model, we evaluate the accuracy and precision of estimating dispersion anisotropy, with the 2-shell optimised protocol [7]. We also assess the consequences of not accounting for dispersion anisotropy, on estimation of the NODDI parameters.

## 2 NODDI Tissue Model

NODDI relates the microstructure parameters to acquired dMRI signals, using a two-level multi-compartment model. At the first level, the signals from the tissue and non-tissue components of the brain are modelled separately, weighted by their respective volume fractions, to obtain the total signal.

The non-tissue compartment represents the free diffusing water in the brain (e.g. CSF and interstitial fluid) and is modelled by isotropic Gaussian diffusion, with diffusivity,  $d_{iso} = 3.0 \times 10^{-9} m^2 s^{-1}$ . The volume fraction of this compartment is denoted by  $\nu_{iso}$  and that of the tissue compartment by  $(1 - \nu_{iso})$ .

The second level models the signal from tissue compartment (grey and white matter (GM/WM)) as a sum of the signal originating from inside the neurites (intra-neurite) and that from the space outside them (extra-neurite), weighted by their respective volume fractions. The intra-neurite volume fraction gives an estimate of neurite density and we denote it by  $\nu_{in}$ , while the extra-neurite volume fraction is  $(1 - \nu_{in})$ . The membrane of neurites restrict the water diffusion to be along their length, so the signal from a neurite is computed as the attenuation due to unhindered diffusion along a stick with diffusivity  $d_{\parallel} = 1.7 \times 10^{-9} m^2 s^{-1}$ . The intra-neurite signal,  $A_{in}$  is:

$$A_{in} = \int_{\mathbb{S}^2} f(\mathbf{n}) e^{-bd_{\parallel}(\mathbf{q}\cdot\mathbf{n})^2} d\mathbf{n}, \tag{1}$$

where  $\mathbf{q}$  and  $b$  are the gradient direction and b-value of the diffusion-weighting, and  $f(\mathbf{n})d\mathbf{n}$  gives the probability of finding sticks along an orientation  $\mathbf{n}$ . The diffusion in the extra-neurite space is hindered by the presence of neurites; thus the orientation distribution of neurites affects the the extra-neurite signal,  $A_{en}$ . Therefore we couple the two tissue compartments by the orientation distribution function  $f(\mathbf{n})$ .  $A_{en}$  is modelled with anisotropic (Gaussian) diffusion:

$$\log A_{en} = -b\mathbf{q}^T \left( \int_{\mathbb{S}^2} f(\mathbf{n}) D(\mathbf{n}) d\mathbf{n} \right) \mathbf{q}, \tag{2}$$

where  $D(\mathbf{n})$  is a cylindrically symmetric tensor. In the present work we use the Bingham distribution as  $f(\mathbf{n})$ , as described in the next section. Hereafter the proposed model will be referred to as Bingham-NODDI, and the original as Watson-NODDI.

## 2.1 Bingham Distribution

The Bingham distribution [10] is a statistical parametric distribution, which is the spherical analogue of the 2-D Gaussian distribution. It quantifies the probability density of orientations along the axes in a 3-D spherical coordinate system. The distribution is characterised by three orthogonal orientations:  $\boldsymbol{\mu}_1$ ,  $\boldsymbol{\mu}_2$  and  $\boldsymbol{\mu}_3$ ; and their respective concentrations,  $\kappa_1 \geq \kappa_2 \geq \kappa_3$ ; as shown in Fig.1.

To simplify the representation, we redefine the concentration parameters as:  $\kappa \geq \beta \geq 0$ , where  $\kappa = (\kappa_1 - \kappa_3)$  and  $\beta = (\kappa_2 - \kappa_3)$ , similarly to [11]. The Bingham distribution is then defined as:

$$f(\mathbf{n}) = F(\kappa, \beta)^{-1} e^{\kappa(\boldsymbol{\mu}_1 \cdot \mathbf{n})^2 + \beta(\boldsymbol{\mu}_2 \cdot \mathbf{n})^2} \quad (3)$$

where  $F$  is a confluent hypergeometric function.

## 2.2 Orientation Tensor

We summarise the orientation distribution of the neurites in each voxel in terms of an orientation tensor (OT), similar to the 3-D rendering of the diffusion tensors (DT). OT is defined as the scatter matrix (second moment) of an orientation distribution function, such as the Bingham distribution:

$$T_{i,j} = \int_{\mathbb{S}^2} \mathbf{n}_i f(\mathbf{n}) \mathbf{n}_j d\mathbf{n} \quad (4)$$

The primary and secondary eigenvalues of the OT,  $1 \geq \tau_1 \geq 1/3$ ,  $\tau_1 \geq \tau_2 \geq 0$ , are functions of the concentration parameters  $\kappa$  and  $\beta$ , and reflect the relative concentration of neurites along the dominant and primary dispersion orientations, respectively. The corresponding eigenvectors are precisely  $\boldsymbol{\mu}_1$  and  $\boldsymbol{\mu}_2$ .

**Dispersion Anisotropy Index (DAI):** To quantify the dispersion anisotropy of neurites, we use the planarity measure [15] of the OT:  $DAI = \frac{(\tau_2 - \tau_3)}{\tau_1}$ .  $DAI$  is zero for isotropic dispersion about  $\boldsymbol{\mu}_1$  (Watson) and one for maximum anisotropic dispersion, i.e. when  $\tau_1 = \tau_2 = 0.5$ .  $DAI$  is a measure specifically related to the orientation distribution, unlike the planarity measure of a DT, which is influenced by  $DAI$  as well as other features like neurite density.

To quantify the dispersion of neurites, we use  $\tau_1$ , and  $\tau_2$  as they have a finite range, unlike  $\kappa$  and  $\beta$ , which range between 0 and  $\infty$ . The concentration parameter  $\tau_1$  is inversely proportional to the dispersion parameter ODI in the original NODDI model, which is an arbitrary transformation to map  $\kappa$  to a finite range. To determine  $\tau_1$  and  $\tau_2$ , we compute the OT from the estimated values of  $\kappa$ ,  $\beta$ , using the equations 3 and 4 (The tertiary eigenvalue is by definition:  $1 - \tau_1 - \tau_2$ , and can be determined once  $\tau_1$  and  $\tau_2$  are computed). Since eigenvectors are mutually orthogonal, the dominant orientation,  $\boldsymbol{\mu}_1$  and the primary dispersion orientation  $\boldsymbol{\mu}_2$  can be quantified as a 3-D rotation of the coordinate system in which the Bingham distribution is defined. Thus we only need to estimate two extra parameters,  $\beta$  and the angle defining the rotation of the plane orthogonal to  $\boldsymbol{\mu}_1$ , compared to those estimated in Watson-NODDI.

### 3 Experimental Design and Results

We acquire *in vivo* dMRI data for one healthy male, on a 3T Philips scanner ( $G_{max} = 60mT/m$ ), using the 4-shell protocol, as in [7]. We also synthesise data for a range of tissue parameters, to compare estimates against known ground truth, similarly to [7] but using the Bingham distribution.

The NODDI Matlab toolbox<sup>1</sup> is modified to incorporate the Bingham distribution, which is then fit to the *in vivo* and synthetic data. To assess the influence of using a simplified model to represent the neurite orientation distribution, we also fit Watson-NODDI to the data. We use Bayesian Information Criteria (BIC), a standard model selection tool, to determine which model explains the data better, while accounting for the complexity of the models. We use the optimised NODDI protocol, which is a 2-shell subset of the acquired protocol, to assess the performance of the two models. The complete 4-shell data is used as a pseudo ground-truth to calculate the errors in estimation of the parameters *in vivo*. We quantify the accuracy and precision of the parameters separately for WM and GM. For *in vivo* data, the segmentation of WM, GM and the free water compartment signal is done as described in [7]; ground-truth values of  $\nu_{in}$  are used to do the same for synthetic data.

#### 3.1 Results

Fig. 2 demonstrates the feasibility of *in vivo* estimation of neurite dispersion anisotropy. We show maps of the novel parameters,  $\tau_1$  and DAI (highlighted in yellow) obtained by fitting Bingham-NODDI, for a range of axial slices of the brain. The slices show the cross section of the corona radiata (regions in blue in the RGB map, on either sides of the corpus callosum), a region known to exhibit fanning, as it extends from the internal capsule to the various cortical areas. This fanning is captured by high values of DAI and have a good contrast to the corpus callosum, where neurites are coherently oriented. Such a contrast can not be captured by Watson-NODDI. The last two columns of Fig.2 show the maps of BIC, which clearly show that Bingham-NODDI explains the data better than Watson-NODDI without overfitting. This is consistent with the comparison of models with dispersion in [16]. Watson-NODDI performs worst specifically in areas of high dispersion anisotropy.

Table 1 shows a quantitative analysis of errors in estimation of the parameters from Bingham-NODDI and Watson-NODDI, using the 2-shell NODDI protocol. The estimation errors are very small for Bingham-NODDI estimates showing that we can accurately model dispersion anisotropy using the 2-shell clinical protocol. We also observe that the error and variability associated with  $\mu_2$  estimation is higher than those for  $\mu_1$ , implying that  $\mu_2$  is harder to estimate. A key finding here is that Watson-NODDI can accurately capture neurite morphology in regions of simple neurite configurations, as the errors associated with Watson-NODDI estimates are comparable to those of Bingham-NODDI. These findings are all backed by the synthetic data analysis (results not shown).

<sup>1</sup> [http://nitrc.org/projects/noddi\\_toolbox](http://nitrc.org/projects/noddi_toolbox)

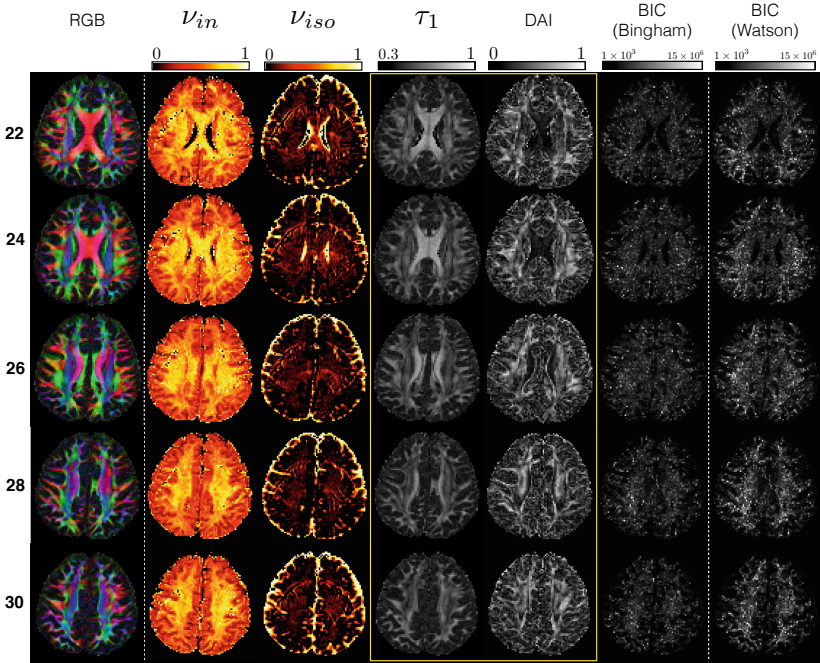


**Fig. 2.** Maps of the novel parameters  $\tau_1$  and DAI (highlighted in yellow), obtained from fitting Bingham-NODDI to *in vivo* data, with estimates of  $\nu_{in}$ ,  $\nu_{iso}$  (columns 2 & 3). Corresponding RGB maps of FA weighted dominant orientation are shown for comparison. The last two columns show the maps of BIC for fitting Bingham-NODDI and Watson-NODDI.

**Table 1.** Mean errors with the corresponding standard deviations of those errors, for estimation of neurite parameters using Bingham-NODDI and Watson-NODDI, with respect to the 4-shell protocol estimates, for *in vivo* data

	Grey Matter		White Matter	
	Bingham	Watson	Bingham	Watson
$\nu_{in}$	-0.025 ± 0.083	-0.025 ± 0.083	-0.002 ± 0.042	-0.001 ± 0.042
$\nu_{iso}$	0.000 ± 0.032	0.001 ± 0.032	0.005 ± 0.029	0.005 ± 0.030
$\tau_1$	0.006 ± 0.038	0.009 ± 0.039	-0.001 ± 0.041	0.000 ± 0.043
$\tau_2$	0.000 ± 0.028	-0.055 ± 0.045	0.003 ± 0.029	-0.074 ± 0.047
$\mu_1$	21.063 ± 21.458	19.709 ± 20.201	5.519 ± 7.430	5.348 ± 6.589
$\mu_2$	27.822 ± 23.521	-	12.002 ± 14.679	-
DAI	0.011 ± 0.122	-	0.010 ± 0.078	-

## 4 Discussion

We demonstrate that it is possible to estimate dispersion anisotropy of neurites *in vivo*, and we can obtain sensible maps of this measure using a clinically feasible protocol. We present DAI as a measure of dispersion anisotropy which is specifically related to the orientation distribution. We show that Bingham-NODDI explains the dMRI signal better than Watson-NODDI, however presence of dispersion anisotropy does not have significant affect on the estimation of dispersion along the dominant orientation. Thus the studies based on the current implementation of NODDI are valid, but Bingham-NODDI may be used to extract parameters for dispersion anisotropy, which can enhance the findings.

A limitation of the method proposed is that it does not explicitly model crossing fibres. But our primary aim is to provide simple and robust microstructure indices and attempting to resolve multiple fibre populations will introduce instability in the model, as shown in [11]. Nevertheless, the model correctly identifies crossing regions with high orientation dispersion and some with high DAI. In future we would like to investigate the possibility of incorporating crossing fibres in Bingham-NODDI. The primary dispersion orientation is found to be harder to estimate than the dominant orientation, which is not unexpected since it represents a more subtle microstructure feature. The estimation of this feature can be improved by increasing the angular resolution of the acquisition protocol. This is not yet clinically feasible with the existing imaging sequences, but emerging technologies, such as multi-band imaging [17], will make it possible to acquire substantially more data per unit time. A reproducibility study is a natural next step for future work, as it will allow to assess if the variability in estimates is low enough to capture between-subject differences. This has implications for use of the technique in disease progression as well as tractography studies. Further work in understanding the relationship between changes in the dispersion anisotropy and normal brain development or pathology, could lead to the measure being utilised as a marker for brain disorders.

**Acknowledgements.** This work is supported by the EPSRC Doctoral Training Award, the MS society in the UK, and the Department of Healths NIHR Biomedical Research Centres funding scheme.

## References

1. Conel, J.L.: The postnatal development of the human cerebral cortex. Harvard University Press, Cambridge (1939)
2. Jacobs, B., Schall, M., Prather, M., Kapler, E., Driscoll, L., Baca, S., Jacobs, J., Ford, K., Wainwright, M., Trembl, M.: Regional dendritic and spine variation in human cerebral cortex: a quantitative Golgi study. *Cerebral Cortex* 11, 558–571 (2001)
3. Fiala, J.C., Spacek, J., Harris, K.M.: Review: Dendritic spine pathology: Cause or consequence of neurological disorders. *Brain Research Reviews* 39, 29–54 (2002)
4. Basser, P.J., Mattiello, J., LeBihan, D.L.: MR diffusion tensor spectroscopy and imaging. *Biophysical Journal* 66, 259–267 (1994)

5. Jespersen, S.N., Kroenke, C.D., Østergaard, L., Ackerman, J.J.H., Yablonskiy, D.A.: Modeling dendrite density from magnetic resonance diffusion measurements. *NeuroImage* 34, 1473–1486 (2007)
6. Jespersen, S.N., Bjarkam, C.R., Nyengaard, J.R., Chakravarty, M.M., Hansen, B., Vosegaard, T., Østergaard, L., Yablonskiy, D.A., Nielsen, N.C., Vestergaard-Poulsen, P.: Neurite density from magnetic resonance diffusion measurements at ultrahigh field: Comparison with light microscopy and electron microscopy. *NeuroImage* 49, 205–216 (2010)
7. Zhang, H., Schneider, T., Wheeler-Kingshott, C.A.M., Alexander, D.C.: NODDI: Practical *in vivo* neurite orientation dispersion and density imaging of the human brain. *NeuroImage* 61, 1000–1016 (2012)
8. Winston, G.P., Micallef, C., Symms, M.R., Alexander, D.C., Duncan, J.S., Zhang, H.: Advanced diffusion imaging sequences could aid assessing patients with focal cortical dysplasia and epilepsy. *Epilepsy Research* 108, 336–339 (2014)
9. Kunz, N., Zhang, H., Vasung, L., O'Brien, K.R., Assaf, Y., Lazeyras, F., Alexander, D.C., Hüppi, P.S.: Assessing white matter microstructure of the newborn with multi-shell diffusion MRI and biophysical compartment models. *NeuroImage* 96, 288–299 (2014)
10. Mardia, K.V., Jupp, P.E.: Directional statistics. Wiley series in probability and statistics. John Wiley & Sons, Ltd. (1990)
11. Sotiropoulos, S.N., Behrens, T.E., Jbabdi, S.: Ball and rackets: Inferring fiber fanning from diffusion-weighted MRI. *NeuroImage* 60, 1412–1425 (2012)
12. Jespersen, S.N., Leigland, L.A., Cornea, A., Kroenke, C.D.: Determination of axonal and dendritic orientation distributions within the developing cerebral cortex by diffusion tensor imaging. *IEEE Transactions in Medical Imaging* 31, 16–32 (2012)
13. Rowe, M.C., Zhang, H., Oxtoby, N., Alexander, D.C.: Beyond crossing fibers: Tractography exploiting sub-voxel fibre dispersion and neighbourhood structure. In: Gee, J.C., Joshi, S., Pohl, K.M., Wells, W.M., Zöllei, L. (eds.) IPMI 2013. LNCS, vol. 7917, pp. 402–413. Springer, Heidelberg (2013)
14. Kaden, E., Knösche, T.R., Anwender, A.: Parametric spherical deconvolution: Inferring anatomical connectivity using diffusion MR imaging. *NeuroImage* 37, 474–488 (2007)
15. Westin, C.-F., Maier, S.E., Mamata, H., Nabavi, A., Jolesz, F.A., Kikinis, R.: Processing and visualization for diffusion tensor MRI. *Medical Image Analysis* 6, 93–108 (2002)
16. Ferizi, U., Schneider, T., Tariq, M., Wheeler-Kingshott, C.A.M., Zhang, H., Alexander, D.C.: The importance of being dispersed: A ranking of diffusion MRI models for fibre dispersion using *in vivo* human brain data. In: Mori, K., Sakuma, I., Sato, Y., Barillot, C., Navab, N. (eds.) MICCAI 2013, Part I. LNCS, vol. 8149, pp. 74–81. Springer, Heidelberg (2013)
17. Feinberg, D.A., Moeller, S., Smith, S.M., Auerbach, E., Ramanna, S., Gunther, M., Glasser, M.F., Miller, K.L., Ugurbil, K., Yacoub, E.: Multiplexed Echo Planar Imaging for sub-second whole brain fMRI and fast diffusion imaging. *PLoS One* 5, e15710 (2010)